Journal of Alloys and Compounds 762 (2018) 21–28

Contents lists available at ScienceDirect

Journal of Alloys and Compounds

journal homepage: http://www.elsevier.com/locate/jalcom

Influences of *in-situ* ZrB_2 and TiB_2 particles on Portevin-Le Chatelier effect for AlSi9Cu1 alloy

H.-S. Yin [a], S.-L. Zhang [a,*], C. Guan [a], Z.-P. Liang [b], Y.-T. Zhao [a], G. Chen [a]

[a] School of Materials Science and Engineering, Jiangsu University, Zhenjiang, Jiangsu, 212013, PR China
[b] Zhenjiang Chuangzhi Special Alloy Technology Development Co. Ltd, Zhenjiang, Jiangsu, 212000, PR China

ARTICLE INFO

Article history:
Received 15 March 2018
Received in revised form
13 May 2018
Accepted 14 May 2018

Keywords:
(TiB_2+ZrB_2)/AlSi9Cu1
In-situ reaction
Portevin-Le Chatelier effect
Critical strain
Tensile test

ABSTRACT

In this paper, the plastic instability phenomenon Portevin-Le Chatelier effect (PLC) was investigated in AlSi9Cu1 alloy and the *in-situ* (ZrB_2+TiB_2)/AlSi9Cu1 composites fabricated from the Al-K_2TiF_6-K_2ZrF_6-KBF_4 system. Microstructure observation and X-ray diffraction testing revealed that the ZrB_2 and TiB_2 particles were generated via direct melting reaction. Mechanical property testing showed that 3 wt.% (ZrB_2+TiB_2) particles reinforced composites owned the highest ultimate tensile strength (226 MPa). Meanwhile, the effects of mass fraction of reinforced particles, strain rate on the critical strain were also systematically studied. The results indicated that both normal and inverse behavior of critical strain *vs.* strain rate existed during the tensile deforming for AlSi9Cu1 alloy and (ZrB_2+TiB_2)/AlSi9Cu1 composites.

1. Introduction

Al-Si-Cu alloy is an important Al-Si alloy and has been widely applied in automobile industries due to its comprehensive properties [1,2]. It is easy to form small-size and dispersed $CuAl_2$ with the addition of copper atoms into Al-Si alloy, which can greatly improve the mechanic properties. However, undesirable platelet-like Si particles and coarse α-Al dendrites may also exist, which deteriorate the mechanical properties especially the ductility and thus limit its industry application [3]. To improve the mechanical and functional properties, particle reinforced aluminum matrix composites (PRAMCs) have gained an increasing interest for structural application in modern industries [4,5]. Various reinforcements, such as SiC, TiC, TiB_2, Al_3Ti, ZrB_2, etc., have been chosen to fabricate aluminum matrix composites [6–9]. Among them, TiB_2 and ZrB_2 are regarded as the ideal reinforcements due to their high strength, good wear resistance and grain refinement effects [10,11].

Most aluminum alloys often exhibit serrations on their stress-strain curves in a given range of temperature and applied strain rate. The occurrence of such serration was first referred as Portevin-Le Chatelier effect (PLC effect) in the beginning of 20th century [12]. Many other experimental observations of PLC effect had been carried out following this early article, mainly in Al-Cu [13], Al-Mg [14], Al-Si [15], or in Al-Li [16] alloys. Associated with the PLC effect, the alloys can be strengthened, but have lower ductility and surface marking may be introduced during cold working, which have a bad influence on the application of these alloys. It is commonly accepted that the PLC effect is the result of dynamic strain aging (DSA) due to the interaction between solute atoms and moving dislocations [17]. According to the classical Cottrell contribution [18], DSA is considered to result from the interaction between bulk diffusion of solute atoms and moving dislocations during plastic deformation. However, researchers found that the pipe diffusion, which is mainly responsible for DSA, is too slow in the absence of excess vacancies [20]. McCormick [17] and Beukel [19] suggested that solute-dislocation interaction occurs mainly at the obstacles where dislocations are temporarily arrested. The obstacles are thought to be grain boundaries and/or forest dislocations [17,20]. DSA is generally seen at intermediate temperatures in the alloys containing interstitial or substitution elements. However, no such behavior was reported in the (ZrB_2+TiB_2)/AlSi9Cu1 matrix composites before. There are many factors can affect the PLC effect, such as testing temperature, applied strain rate and precipitations in

* Corresponding author.
E-mail addresses: 1014409335@qq.com (H.-S. Yin), zsl@ujs.edu.cn (S.-L. Zhang).

https://doi.org/10.1016/j.jallcom.2018.05.164
0925-8388/

alloys. As mentioned above, dislocations play a vital role in dynamic strain aging, since the rigid particles can affect the motion of dislocations, it is assumed that particles also have a vital influence on PLC effect.

The present work is based on such assumption that the addition of reinforced particles to alloys exhibiting the PLC effect can have a significant influence on the unstable deformation. Plastic instability in AlSi9Cu1 alloy and (ZrB_2+TiB_2) particles reinforced AlSi9Cu1 composites were studied experimentally. To better understand the influence of different mass fractions of reinforced particles (0, 1, 2, 3, 5 wt.%) on PLC effect, the critical conditions for plastic instability under strain rate $1.11 \times 10^{-3}s^{-1}$ were analyzed. The critical strain of AlSi9Cu1 alloy and 3 wt.% (ZrB_2+TiB_2)/AlSi9Cu1 composite under strain rate from $1.39 \times 10^{-4}s^{-1}$ to $1.33 \times 10^{-2}s^{-1}$ were also analyzed.

2. Experimental

2.1. Preparation of the in-situ (ZrB_2+TiB_2)/AlSi9Cu1 composites

The (ZrB_2+TiB_2)/AlSi9Cu1 composites were fabricated from the Al-K_2TiF_6-K_2ZrF_6-KBF_4 system by melting in-situ technology. AlSi9Cu1 alloy was cast from industrial pure aluminum (99.50%), Al-20Si master alloy and electrolytic copper. The alloy was firstly melted in the electromagnetic induction furnace at 860 °C and then powder reactants wrapped with aluminum foil were pressed into the melting alloy. Reaction time was 25–35 min, the melt alloy was refined and degassed with C_2Cl_6. After slagging-off, the melt was cast to copper module and cooled to the room temperature (RT). The chemical compositions of the AlSi9Cu1 alloy, determined via emission spectroscopy, are given in Table 1.

2.2. Mechanical testing

Tensile specimens cut out from the same position of casting composites had a gauge length of 15 mm with a cross section of 4×2 mm^2 as shown in Fig. 1. Tensile tests were carried out with an electronic tensile testing machine (AGS-X) at room temperature under strain rate from $1.39 \times 10^{-4}s^{-1}$ to $1.33 \times 10^{-2}s^{-1}$. Three tensile specimens were tested for each condition.

2.3. Microstructural analysis

The microstructures of the alloys and composites were examined by an optical microscopy (OM, LEICA-DM-2500 M) and scanning electron microscope (SEM, JEOL JSM-7001 F). The X-ray diffraction (DMAX 2500 PC) with Cu Kα radiation was used to determine the particles and phases component.

3. Results and discussion

3.1. Microstructure of composites

Fig. 2 shows the XRD pattern of the (ZrB_2+TiB_2)/AlSi9Cu1 composite fabricated from the Al-K_2TiF_6-K_2ZrF_6-KBF_4 system by in-situ reaction technology. The diffraction peaks of ZrB_2, TiB_2, $CuAl_2$,

Table 1
Chemical composition of the AlSi9Cu1 alloy (in wt.%).

Element	Si	Cu	Fe	Mn	Al
Content	8.61	0.949	0.238	0.097	Balance

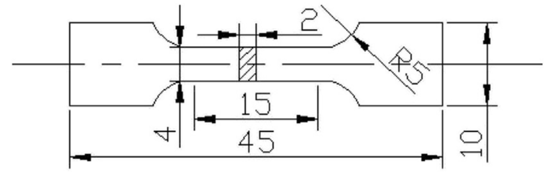

Fig. 1. Size of the specimens for tensile test.

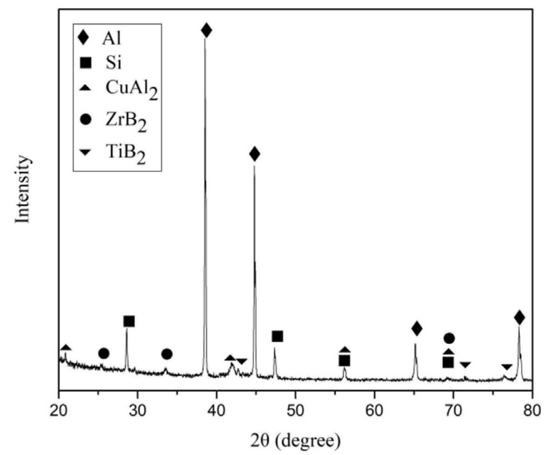

Fig. 2. XRD pattern of (ZrB_2+TiB_2)/AlSi9Cu1 matrix composites.

Si and α-Al phases are clearly observed, respectively. According to Ref. [21], the overall reaction can be illustrated as follows:

$$3K_2ZrF_6 + 3K_2TiF_6 + 12KBF_4 + 20Al = 3ZrB_2 + 3TiB_2 + 18KAlF_4 + 2K_3AlF_6 \quad (1)$$

Fig. 3 gives the SEM images of the (ZrB_2+TiB_2)/AlSi9Cu1 composites with different mass fraction particles. As shown in Fig. 3, the in-situ (ZrB_2+TiB_2) particles are distributed as reinforced clusters and strip-like clusters in the aluminum matrix. The quantity and size of reinforced clusters changed with the increasing of the particles mass fraction. The average size of reinforced clusters increased from 9.5 μm to 27.3 μm due to the particles mass fraction increasing from 1 wt.% to 5 wt.%. Especially, when the particles mass fraction was 3 wt.%, the quantity and the size of the reinforced clusters are the most appropriate. However, when the particles mass fraction reached to 5 wt.%, the size of the reinforced clusters reached to 42.6 μm. These large-sized clusters lead to serious stress concentration, and the strength and ductility of the composites decreased.

The highly magnified SEM images, EDS spectrum and size distribution of (ZrB_2+TiB_2) particles in the (ZrB_2+TiB_2)/AlSi9Cu1 composite are presented in Fig. 4. It can be easily observed that most of the ZrB_2 and TiB_2 particles are in a relatively dispersed state within the local area in Fig. 4 (c). The ZrB_2 and TiB_2 exhibit spherical, hexagonal and cubic shapes. Combining with the XRD analysis of the composites in Fig. 2 and EDS analysis of the reinforcement which is mainly consisted of Zr, Ti and B elements in Fig. 4 (b), the nanoparticles are ZrB_2 and TiB_2. Fig. 4 (c) and (d) illustrate that the particles separate from each other in local area. The size is in the range of 10–160 nm, and the average size is 65 nm.